

# blood

2010 116: 3185-3196  
Prepublished online Jul 14, 2010;  
doi:10.1182/blood-2009-12-260703

## Phenotypically identical hemopoietic stem cells isolated from different regions of bone marrow have different biologic potential

Jochen Grassinger, David N. Haylock, Brenda Williams, Gemma H. Olsen and Susan K. Nilsson

---

Updated information and services can be found at:  
<http://bloodjournal.hematologylibrary.org/cgi/content/full/116/17/3185>

Articles on similar topics may be found in the following *Blood* collections:  
[Hematopoiesis and Stem Cells](#) (2766 articles)

---

Information about reproducing this article in parts or in its entirety may be found online at:  
[http://bloodjournal.hematologylibrary.org/misc/rights.dtl#repub\\_requests](http://bloodjournal.hematologylibrary.org/misc/rights.dtl#repub_requests)

Information about ordering reprints may be found online at:  
<http://bloodjournal.hematologylibrary.org/misc/rights.dtl#reprints>

Information about subscriptions and ASH membership may be found online at:  
<http://bloodjournal.hematologylibrary.org/subscriptions/index.dtl>



# Phenotypically identical hemopoietic stem cells isolated from different regions of bone marrow have different biologic potential

Jochen Grassinger,<sup>1,2</sup> David N. Haylock,<sup>2,3</sup> Brenda Williams,<sup>3</sup> Gemma H. Olsen,<sup>3</sup> and Susan K. Nilsson<sup>2,3</sup>

<sup>1</sup>Australian Stem Cell Centre, Clayton, Australia; <sup>2</sup>Department of Anatomy and Developmental Cell Biology, Monash University, Clayton, Australia; and <sup>3</sup>CSIRO Materials Science and Engineering (CMSE), Commonwealth Scientific and Industrial Research Organisation (CSIRO), Clayton, Australia

**Hemopoietic stem cells (HSCs) reside within a specified area of the bone marrow (BM) cavity called a “niche” that modulates HSC quiescence, proliferation, differentiation, and migration. Our previous studies have identified the endosteal BM region as the site for the HSC niche and demonstrated that hemopoietic stem and progenitor populations (HSPCs, LSK) isolated from different BM regions exhibit significantly different hemopoietic potential. In this study, we have**

**analyzed subpopulations of LSK cells isolated from different regions of the BM and showed that CD150<sup>+</sup>CD48<sup>-</sup>LSK HSCs within the endosteal BM region have superior proliferative capacity and homing efficiency compared with CD150<sup>+</sup>CD48<sup>-</sup>LSK HSCs isolated from the central BM. Furthermore, we show, for the first time, that a subset of CD150<sup>+</sup>CD48<sup>+</sup>LSK progenitor cells, previously defined as B-lymphoid primed hemopoietic cells, are capable of multilineage reconstitution, however, only**

**when isolated from the endosteal region. In addition, we provide evidence for an unrecognized role of CD48 in HSC homing. Together, our data provide strong evidence that highly purified HSCs show functional differences depending on their origin within the BM and that the most primitive HSCs reside within the endosteal BM region. (*Blood*. 2010;116(17):3185-3196)**

## Introduction

Definitive hemopoiesis in adult mammals is restricted to bone marrow (BM) where specialized microenvironments attract circulating hemopoietic stem cells (HSCs) during embryogenesis and in adults. The HSC niche is composed of extracellular matrix proteins, growth factors, chemokines, and cells.<sup>1</sup>

The hierarchy of HSCs has been extensively studied using animal models analyzing the reconstitution ability of phenotypically distinct subsets after transplantation. Hemopoietic stem and progenitor populations (HSPCs) can be defined as: long-term (LT) HSCs with multilineage engraftment potential and unlimited population self-renewal potential; short-term (ST) HSCs with transient multilineage reconstitution potential and multipotent progenitors that do not self-renew but give rise to myeloid and lymphoid cells.<sup>2</sup> Multiparametric cell sorting allows selective enrichment of HSPC subpopulations to be tested in limiting dilution or single-cell transplantations. Early experiments suggested lineage-negative (Lin<sup>-</sup>) BM expressing c-kit and Sca (LSK) are enriched for HSPCs.<sup>3</sup> LSK represent approximately 0.05% of nucleated BM, containing progenitors and LT-HSC, not expressing CD34 or CD135.<sup>4,5</sup> Transplantations with HSCs, further fractionated with SLAM markers, demonstrated that 1 in 2.2 single-sorted CD150<sup>+</sup>CD41/48<sup>-</sup>Lin<sup>-</sup> cells are LT-HSCs.<sup>6</sup>

Despite defining the phenotype of LT-HSCs, the exact location of these cells within BM remains contentious. Extensive data from multiple laboratories, including ours, suggest the endosteal region plays a key role in regulating hemopoiesis and the HSC pool.<sup>7-21</sup>

We recently demonstrated endosteal HSPCs have superior hemopoietic potential compared with central HSPCs.<sup>22</sup> Therefore, we hypothesize that endosteal LT-HSCs (LSKCD150<sup>+</sup>CD41/

48<sup>-</sup>Lin<sup>-</sup>) will also exhibit different biologic properties compared with their central counterparts.

In this study, we functionally characterized subpopulations within the HSPC pool isolated from these locations. Herein, we show that proliferation *in vitro*, and homing efficiency and spatial distribution after transplantation, is dependent on the location from which cells were isolated. We provide data highlighting the importance of CD48 in cell homing, and using competitive transplantation assays show that endosteal CD150<sup>+</sup>CD48<sup>+</sup>LSK (endCD150<sup>+</sup>CD48<sup>+</sup>LSK) contain a subset of HSCs with previously unrecognized multilineage long-term repopulation potential.

## Methods

### Mice

C57BL/6 (C57) and PTPRCA mice were bred at Monash Animal Services (Monash University, Clayton, Australia). Red fluorescent protein (RFP) mice were provided by Professor Patrick Tam (Children's Medical Research Institute, Sydney, Australia). Mice were 6 to 8 weeks old and sex-matched for experiments. Irradiation was done in a split dose (5.25 Gy each) 6 hours apart, 24 hours before transplantation. A total of 2 × 10<sup>5</sup> unlabeled irradiated (15 Gy) C57 BM was used as carrier cells for every recipient. All experiments were approved by Monash Animal Services ethics committee.

### Hemopoietic cell isolation

Populations of HSCs/HPCs were isolated as previously described.<sup>18</sup> Briefly, femurs, tibia, and iliac crests were excised, the epiphyseal and metaphyseal

Submitted December 22, 2009; accepted June 24, 2010. Prepublished online as *Blood* First Edition paper, July 14, 2010; DOI 10.1182/blood-2009-12-260703.

The online version of this article contains a data supplement.

The publication costs of this article were defrayed in part by page charge payment. Therefore, and solely to indicate this fact, this article is hereby marked “advertisement” in accordance with 18 USC section 1734.

© 2010 by The American Society of Hematology

regions removed as previously described,<sup>23</sup> and bones flushed to isolate central BM. Flushed bones and epiphyseal and metaphyseal ends were pooled, ground using a mortar and pestle, and endosteal cells collected. Bone fragments were digested with collagenase I (3 mg/mL) and dispase II (4 mg/mL) at 37°C in an orbital shaker. The fragments were washed to isolate residual endosteal cells and both endosteal fractions pooled. Materials are available as a kit (SCR051; Millipore). Mononuclear cells were enriched using density centrifugation (Nycoprep; Axis-Shield) according to the manufacturer's instructions and labeled with a cocktail of anti-mouse antibodies: B220 (CD45R), Mac-1 (CD11b), Gr-1 (Ly-6G), and Ter119 (BD Biosciences PharMingen). Lin<sup>-</sup> cells were obtained using anti-rat Dynal beads (Invitrogen) according to the manufacturer's instructions and cells stained for flow cytometry. Peripheral blood (PB) was collected by retro-orbital puncture. Red blood cells were lysed using ammonium chloride.

### Flow cytometry

Flow cytometric analysis was performed using an LSR II (BD Biosciences), as previously described.<sup>18</sup> Cells were immunolabeled with a lineage cocktail (CD3, CD4, CD8, CD41, Ter-119, Gr-1, Mac-1, and B220) and anti-Sca-1-PECy7, anti-CD150-phycoerythrin, anti-CD48-Pacific Blue, and anti-c-kit-allophycocyanin antibodies. For BM and PB, typically  $5 \times 10^5$  and 1 to  $3 \times 10^5$  events, respectively, were analyzed at approximately 10 000 events per second. Cells were sorted at approximately 8000 events per second and reanalyzed for purity on a Cytospea Influx as previously described.<sup>18</sup> Antibody combinations were chosen to minimize emission spectra overlap (supplemental Tables 1-2, available on the *Blood* Web site; see the Supplemental Materials link at the top of the online article).

### CFDA-SE and SNARF staining

Cells were stained with 5-(and 6-)carboxyfluorescein diacetate succinimidyl ester (CFDA-SE) or seminaphthorhodafluor-1-carboxylic acid acetate succinimidyl ester (SNARF; Invitrogen) at a final concentration of 0.5  $\mu$ M and 1  $\mu$ M, respectively, as previously described.<sup>24</sup> Briefly, populations were stained in phosphate-buffered saline (PBS) supplemented with 0.5% bovine serum albumin at 37°C. After 10 minutes, staining was quenched with ice-cold PBS 20% Se, the cells washed twice with PBS 2% Se, and staining confirmed using fluorescence microscopy.

### Proliferation assay

Fifty cells were sorted into each of 5 replicate wells of a 96-well flat bottom culture plate into serum-free Iscove modified Dulbecco medium (Invitrogen) supplemented with mouse stem cell factor (SCF; Millipore), human FLT-3 ligand (FL), and human interleukin-6 (IL-6) and IL-11 (all Pepro-Tech) as previously described.<sup>22</sup> After 6 days, cells were harvested, counted, and stained with antibodies to Sca, c-kit, B220, Gr-1, and Mac-1 for flow cytometric analysis.

### Homing and spatial distribution assay

The homing efficiency and spatial distribution of endosteal or central, CFDA-SE<sup>+</sup> or SNARF<sup>+</sup>, LSK or CD150<sup>+</sup>CD48<sup>+/−</sup>LSK cotransplanted with carrier cells into ablated or nonablated recipients was determined. Approximately 1 to  $3 \times 10^3$  CD150<sup>+</sup>CD48<sup>-</sup>LSK, 1 to  $5 \times 10^3$  CD150<sup>+</sup>CD48<sup>+</sup>LSK, and 1 to  $5 \times 10^4$  LSK were injected. Endosteal CFSE<sup>+</sup> and central SNARF-1<sup>+</sup> (or vice versa) cells were transplanted into the same recipients to exclude injection-related variability. After 15 hours, 1 iliac artery was ligated after laparotomy and the leg removed. BM was isolated by grinding and digestion of bone fragments with collagenase and dispase without prior flushing, as described in "Hemopoietic cell isolation." The white blood cell number was determined (Sysmex) and used as the denominator for subsequent statistical analysis. Flow cytometry was used for analysis of SNARF-1<sup>+</sup> and CFSE<sup>+</sup> cells. To ensure 50 to 100 positive events, 1 to  $2.5 \times 10^7$  cells were analyzed within the white blood cell gate. The homing efficiency was expressed as the percentage of injected cells assuming 1 femur, tibia, and iliac bone represents 15% of total BM mass.<sup>18</sup>

The second leg was perfused with 4% paraformaldehyde at physiologic pressure through the caudal aorta, the femur excised and decalcified using 10% ethylenediamine tetraacetic acid (Sigma-Aldrich). Sections were cut and analyzed for spatial distribution as previously described.<sup>24</sup>

### Functional selection of LT-HSC and limiting dilution reconstitution

Endosteal LSK from 10 RFP donors were transplanted into a single nonablated C57 recipient. After 5 hours, the recipient endosteal BM was harvested as described in "Hemopoietic cell isolation" and donor RFP LSK within the endosteal region reisolated. Endosteal homed RFP<sup>+</sup> LSK were transplanted in a limiting dilution assay (3, 10, 30, and 100 cells) into irradiated secondary C57 recipients. In a second series of experiments, endosteal LSK were transplanted in limiting dilution (30, 100, 300, and 1000 cells per group) into irradiated C57 recipients.

For all transplantations, PB reconstitution was assessed after 6, 12, and 20 weeks and BM after 20 weeks. Cells were stained with anti-Gr-1-fluorescein isothiocyanate (FITC), anti-Mac-1-FITC, anti-B220-FITC, anti-B220-Pacific Blue, anti-CD3-Pacific Blue antibodies or anti-Gr-1-FITC, anti-Mac-1-FITC, and anti-B220-phycoerythrin antibodies. Mice with donor lymphoid and myeloid reconstituted were designated as multilineage. The frequency of multilineage donor contribution was calculated using L-Calc (StemCell Technologies).

### Competitive limiting dilution reconstitution assay

In additional experiments, the multilineage reconstitution potential of endosteal and central CD150<sup>+</sup>CD48<sup>-</sup>LSK and CD150<sup>+</sup>CD48<sup>+</sup>LSK subpopulations was assessed using competitive limiting dilution transplantations (20, 100, 200, and 500 PTPRCA CD150<sup>+</sup>CD48<sup>+</sup>LSK isolated from each region competed with 200 [transplantation 1] or 150 [transplantation 2] RFP CD150<sup>+</sup>CD48<sup>-</sup>LSK isolated from the same BM region) into irradiated secondary C57 recipients.

In other experiments, the hemopoietic potential of endCD150<sup>+</sup>CD48<sup>+</sup>LSK and central CD150<sup>+</sup>CD48<sup>+</sup>LSK (centCD150<sup>+</sup>CD48<sup>+</sup>LSK) was assessed using limiting dilution transplantations (30, 100, 300, and 1000 RFP endCD150<sup>+</sup>CD48<sup>+</sup>LSK competed with 300 PTPRCA centCD150<sup>+</sup>CD48<sup>+</sup>LSK) into irradiated secondary C57 recipients.

For all transplantations, PB reconstitution was assessed after 6, 12, and 20 weeks and BM after 20 weeks, as described in the previous subsection. Cells were stained with antibodies to CD45.1-allophycocyanin (PTPRCA donor), CD45.2-PeCy5.5 (RFP donor and host), B220-Pacific Blue and B220-FITC (B cells), CD3-Pacific Blue (T cells), Gr-1-FITC, and Mac-1-FITC (myeloid).

### Cell-cycle analysis

Sorted endCD150<sup>+</sup>CD48<sup>-</sup>LSK and centCD150<sup>+</sup>CD48<sup>-</sup>LSK were fixed and permeabilized by dropping them into 70% ethanol. Consequently, cells were washed twice with PBS and stained with 1 mg/mL propidium iodide (Invitrogen) and 200  $\mu$ g/mL RNase A (QIAGEN) for 30 minutes at 37°C. Cells were immediately analyzed by flow cytometry for DNA staining using an LSR II.

### Statistical analysis and data presentation

Flow cytometric analysis was performed using FlowJo software Version 9.1. Where appropriate, a Student *t* test or an analysis of variance in conjunction with a Newman-Keuls test was used to determine statistical significance.

## Results

### LT-HSC (CD150<sup>+</sup>CD48<sup>-</sup>LSK) incidence is equivalent in endosteal and central BM

Our previous studies demonstrate that C57 endosteal LSK exhibit superior hemopoietic function and potential compared with their

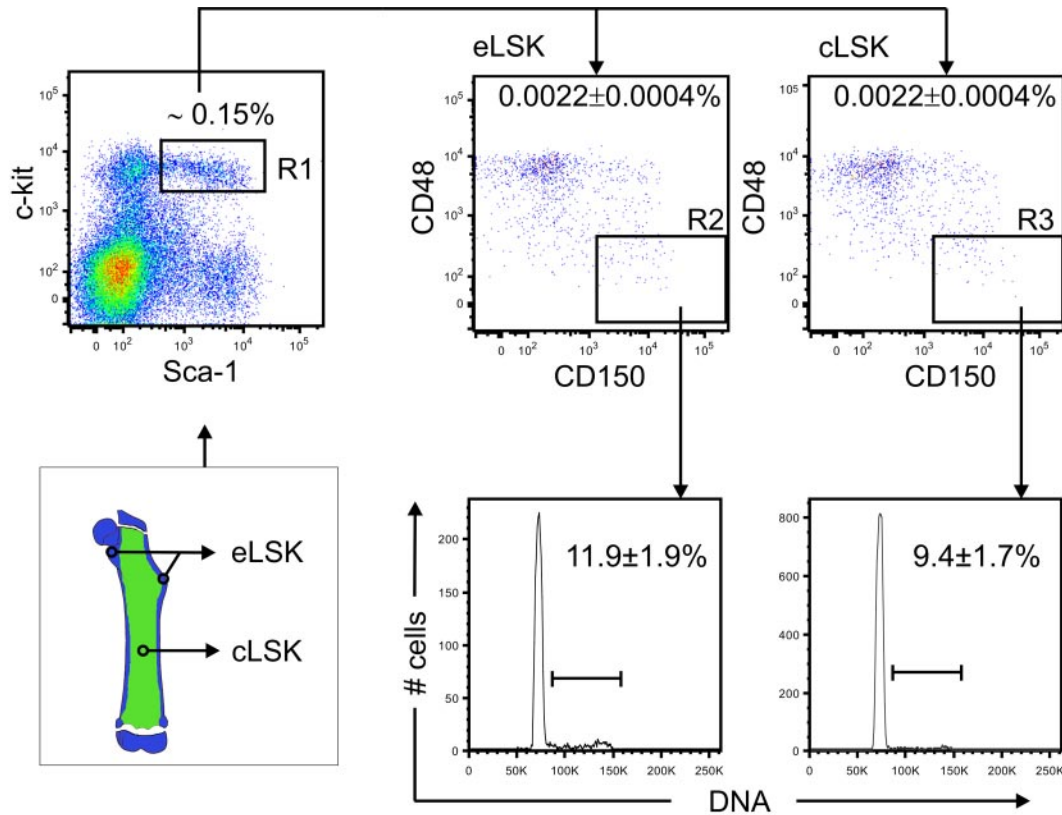


**Figure 1. Distribution and cell-cycle state of endosteal and central CD150<sup>+</sup>CD48<sup>-</sup>LSK.** WBM stained with anti-Sca-1, c-kit, CD150, and CD48. Dot plots show a representative analysis of CD150 and CD48 expression on endosteal (eLSK) and central (cLSK) BM (both gated for R1). Values are the mean ± SEM (5 animals). Histograms show a representative analysis of endosteal (R2) and central (R3) CD150<sup>+</sup>CD48<sup>-</sup>LSK stained with propidium iodide to determine the proportion of cycling cells. Data are the mean of 3 individual experiments ± SEM.

central counterparts.<sup>22</sup> Specifically, significantly increased multilineage engraftment was detected when endosteal LSK were competed with central LSK in long-term limiting dilution transplantations. However, it is well known that LSK are a heterogeneous pool of LT-HSCs, ST-HSCs, and multipotent progenitors and the increased frequency of repopulating cells in endosteal BM could simply be the result of a higher incidence of LT-HSCs. Using our newly developed harvesting method, specifically isolating endosteal and central fractions, we analyzed the incidence of endosteal and central LSK and CD150<sup>+</sup>CD48<sup>-</sup>LSK. To ensure an accurate discrimination of LT-HSCs, we included Sca and c-kit selection and hierarchically backgated Lin<sup>-</sup>CD150<sup>+</sup>CD48<sup>-</sup> cells (supplemental Figure 1).

Using this gating strategy, we demonstrated that the incidence is not significantly different in the 2 regions (Figure 1). Specifically, 0.2% ± 0.02% and 0.002% ± 0.0004% of endosteal and central BM are LSK (R1) and CD150<sup>+</sup>CD48<sup>-</sup>LSK (R2 and R3, respectively). Assuming that 1 femur, tibia, and iliac bone represents approximately 15% of total nucleated cells<sup>18</sup> and the endosteal and central white blood cell numbers are 116 ± 4 × 10<sup>6</sup> and 385 ± 28 × 10<sup>6</sup>, respectively, then 25 ± 5 × 10<sup>2</sup> and 86 ± 18 × 10<sup>2</sup> CD150<sup>+</sup>CD48<sup>-</sup>LSK reside in the endosteal and central BM, respectively (n = 5). Importantly, these data demonstrate that simply flushing bones results in a significant proportion (~25%) of LT-HSCs being discarded. The prime aim of our subsequent studies was to compare the characteristics and hemopoietic potential of LSK subpopulations isolated from these BM regions.

#### No differences in cell-cycle status were detected between endosteal and central LT-HSCs

Steady-state LT-HSCs are quiescent,<sup>25</sup> and data from our laboratory and others suggest that endosteal HSCs are subject to a number of potent negative regulators, such as ANG-1 and osteopontin.<sup>11,13</sup> To determine whether a higher number of centCD150<sup>+</sup>CD48<sup>-</sup>LSK are in cell cycle compared with endCD150<sup>+</sup>CD48<sup>-</sup>LSK, we performed cell cycle analysis using DNA staining. Interestingly, there was no significant difference in the proportion of endosteal or central CD150<sup>+</sup>CD48<sup>-</sup>LSK in S/G<sub>2</sub>/M phase (12% and 9%, *P* = .71; Figure 1).

#### Endosteal HSCs exhibit higher in vitro proliferative potential while retaining their primitive phenotype

To gain more insight into the biologic properties of endosteal and central LT-HSCs with identical CD150<sup>+</sup>CD48<sup>-</sup>LSK phenotypes, a series of in vitro and in vivo experiments were conducted.

Initially, endosteal and central CD150<sup>+</sup>CD48<sup>-</sup>LSK and CD150<sup>+</sup>CD48<sup>+</sup>LSK were sorted (Figure 2A) and cultured in serum-free medium supplemented with SCF, FL, IL-6, and IL-11 for 6 days to compare proliferation and differentiation. The majority of CD150<sup>+</sup>CD48<sup>-</sup>LSK progeny were dispersed and homogeneous in morphology, whereas in contrast, CD150<sup>+</sup>CD48<sup>+</sup>LSK progeny formed clusters and contained megakaryocyte-progenitor-like cells (supplemental Figure 2). Furthermore, these morphologic differences between the

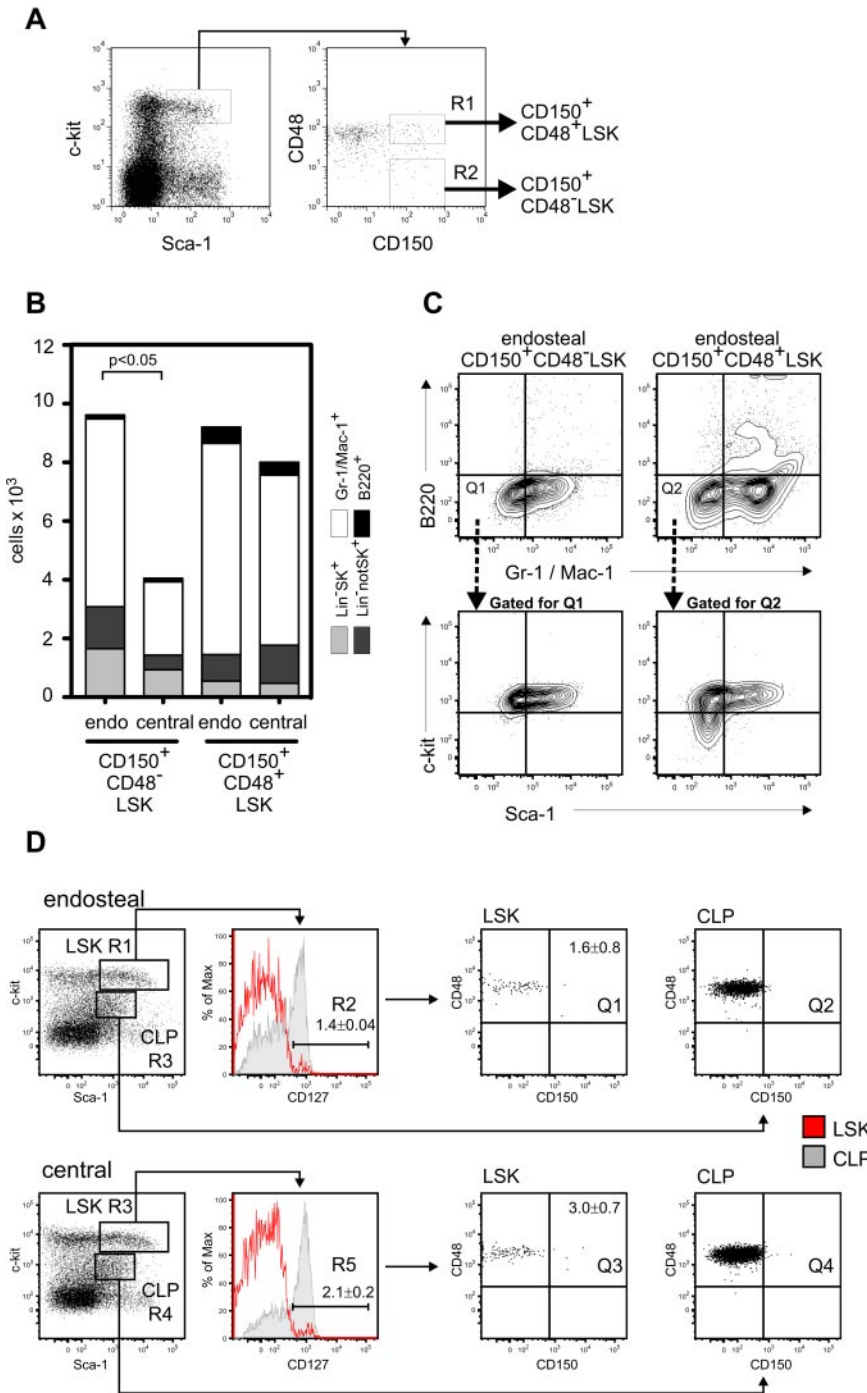


**Figure 2. Central CD150<sup>+</sup>CD48<sup>-</sup>LSK show significantly decreased proliferative potential.** (A) Endosteal and central BM was sorted for CD150<sup>+</sup>CD48<sup>-</sup>LSK (R1) and CD150<sup>+</sup>CD48<sup>+</sup>LSK (R2). Fifty cells were cultured in each of 5 wells in serum-free medium supplemented with SCF, IL-6, IL-11, and FL for 6 days and analyzed for total cell number and expression of Sca-1, c-kit, B220, Gr-1, and Mac-1. (B) Number of progeny with Sca-1<sup>+</sup>c-kit<sup>+</sup>Lin<sup>-</sup>, Sca-1<sup>+</sup>c-kit<sup>-</sup>Lin<sup>-</sup>, B220<sup>+</sup>, and Gr-1/Mac-1<sup>+</sup> phenotypes after 6 days. Lin<sup>-</sup> is defined as Q1/Q2 (C). Bars represent average of 3 experiments. (C) Representative flow cytometric analysis of cultures. Bottom dot plots are gated for Q1 or Q2, respectively, to exclude Gr-1/Mac-1 and B220 expressing cells. (D) Representative flow cytometric analysis of CD127, CD150, and CD48 expression on endosteal and central LSK and common lymphoid progenitors (CLP). Data are mean ± SEM of 2 experiments.

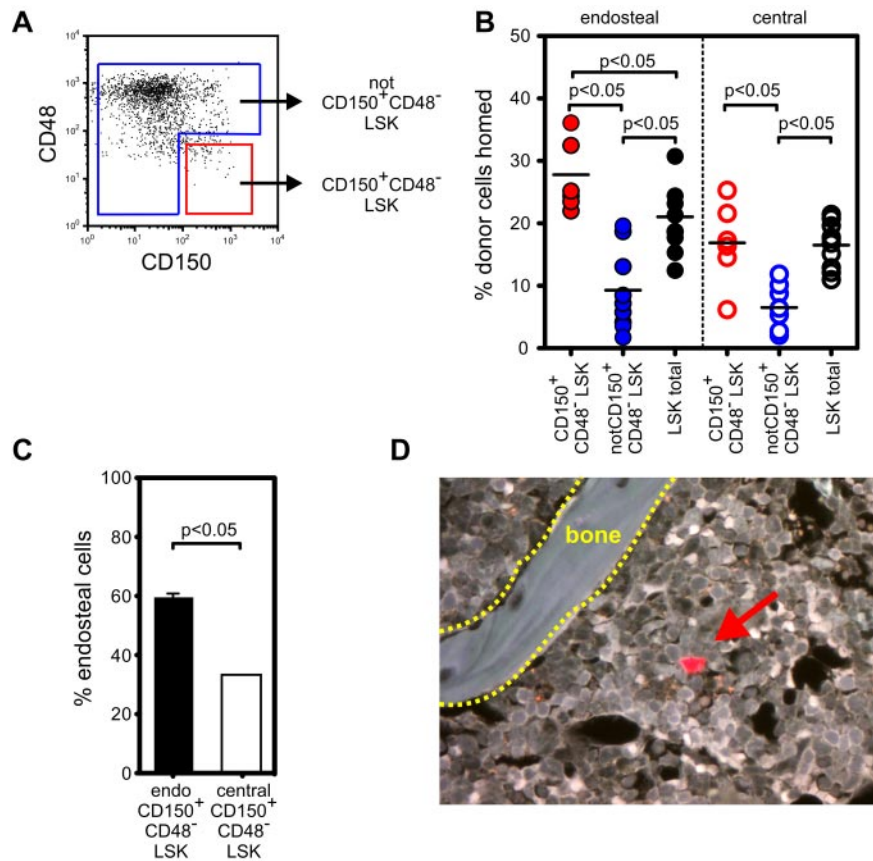
CD150<sup>+</sup>CD48<sup>-</sup>LSK and CD150<sup>+</sup>CD48<sup>+</sup>LSK progeny were consistent for both endosteal and central cells (data not shown).

The total number of progeny derived from endCD150<sup>+</sup>CD48<sup>-</sup>LSK was significantly higher (2.5-fold) than that generated from centCD150<sup>+</sup>CD48<sup>-</sup>LSK ( $10 \pm 1 \times 10^3$  and  $4 \pm 1 \times 10^3$  cells, respectively,  $P < .05$ ; Figure 2B). In addition, flow cytometric analysis demonstrated that CD150<sup>+</sup>CD48<sup>-</sup>LSK generated significantly more progeny with a primitive phenotype compared with CD150<sup>+</sup>CD48<sup>+</sup>LSK (Figure 2B-C), with the latter producing increased numbers of cells expressing Gr-1/Mac-1 and B220. CD150<sup>+</sup>CD48<sup>+</sup>LSK isolated from both regions produced increased numbers of progeny

expressing B220, suggesting the presence of lymphoid progenitors.

To test this hypothesis, IL-7R $\alpha$  (CD127) expression, a cell surface marker on common lymphoid progenitors,<sup>26</sup> was analyzed (Figure 2D). A significantly higher proportion of central LSK expressed CD127 compared with endosteal LSK (2.1% and 1.4%, respectively;  $P < .05$ ). However, no CD127 expression was detected on CD48<sup>-</sup>LSK, and the majority of CD127<sup>+</sup> cells were CD150<sup>-</sup>. Of note, only 1.6% of endosteal and 3.0% of central CD150<sup>+</sup>CD48<sup>+</sup>LSK expressed CD127. These data suggest the presence of a lymphoid primed progenitor cell within the CD150<sup>+</sup>CD48<sup>+</sup>LSK population but not in the CD48<sup>-</sup>LSK population.

**Figure 3. Homing and spatial distribution of LSK populations.** (A) Endosteal and central Lin<sup>-</sup> cells stained with Sca-1, c-kit, CD150, and CD48 (clone HM48.1). Sketch shows sorting strategy. Individual endosteal and central cell populations were stained with CFDA-SE or SNARF-1 and cotransplanted into nonablated recipients. In addition, endosteal and central total LSK not stained with CD150 or CD48 were cotransplanted into nonablated recipients. (B) Homing efficiency was determined 15 hours after transplantation. (C) Spatial distribution of CD150<sup>+</sup>CD48<sup>-</sup> LSK and CD150<sup>+</sup>CD48<sup>+</sup> LSK was determined 15 hours after transplantation. Data are mean  $\pm$  SEM. (D) SNARF labeled CD150<sup>+</sup>CD48<sup>-</sup> LSK homed to endosteal BM. Image was acquired on an Olympus BX51 microscope through a 20 $\times$ /0.70 NA UplanApo objective using a cooled monochrome CCD Optronics Magnafire S99802 camera at 40°C below ambient and Magnafire software. Image brightness was adjusted using Adobe Photoshop.



### CD150<sup>+</sup>CD48<sup>-</sup> LSK harvested from endosteal BM have the highest homing efficiency

Because of the previously described differences in LSK cell engraftment<sup>22</sup> and the proliferative potential of LSK subpopulations in vitro, as described in the previous subsection between cells isolated from endosteal and central BM, we hypothesized that endCD150<sup>+</sup>CD48<sup>-</sup> LSK may have greater hemopoietic potential in vivo. As the engraftment potential of transplanted cells is dependent on their ability to home to the BM, we analyzed the homing efficiency of fluorescently labeled CD150<sup>+</sup>CD48<sup>-</sup> LSK (Figure 3A red sort region) and LSK that do not have the phenotype CD150<sup>+</sup>CD48<sup>-</sup> (Figure 3A blue sort region). Both phenotypes were isolated from endosteal and central BM and each phenotype cotransplanted in a 15-hour homing assay into nonablated recipients (Figure 3B). Of note, more endCD150<sup>+</sup>CD48<sup>-</sup> LSK (28%  $\pm$  2%) homed compared with their central counterparts (19%  $\pm$  2%,  $P < .01$ ). Interestingly, the remaining LSK that were not CD150<sup>+</sup>CD48<sup>-</sup> had significantly reduced homing efficiency (9%  $\pm$  2% and 7%  $\pm$  1% for endosteal and central BM, respectively) compared with total LSK (21%  $\pm$  1% and 17%  $\pm$  1%, respectively;  $P < .05$ ).

### Endosteal and central CD150<sup>+</sup>CD48<sup>-</sup> LSK lodge preferentially within their region of origin

We recently showed that 5 hours after transplantation more than 70% of LSK isolated from the endosteum lodge within endosteal BM, and this did not significantly change up to 15 hours.<sup>22,24</sup> To determine whether CD150<sup>+</sup>CD48<sup>-</sup> LSK also lodge within their region of origin, we analyzed their spatial distribution 15 hours after transplantation. As shown in Figure 3C-D, 60%  $\pm$  1% of endCD150<sup>+</sup>CD48<sup>-</sup> LSK preferentially

lodge within endosteal BM (compared with an expected 25% for random distribution<sup>24</sup>). In contrast, a significantly lower percentage of centCD150<sup>+</sup>CD48<sup>-</sup> LSK (33%  $\pm$  0%;  $P < .05$ ) lodged within endosteal BM.

### LT-HSCs can be functionally selected by their ability to home to the endosteal niche

Based on endosteal LT-HSCs having increased homing efficiency together with our previous observations that endosteal LSK have higher engraftment ability and lodge back within endosteal BM within 5 hours, we hypothesized that these functional abilities can be used as a means of selecting LT-HSCs. Endosteal LSK were transplanted into a single nonablated recipient. After 5 hours, endosteally homed donor LSK were reisolated and transplanted into lethally ablated secondary recipients in a limiting dilution transplantation assay (Figure 4A). The frequency of LT-HSCs was determined by analyzing PB for donor-derived CD3, B220, and Gr-1/Mac-1<sup>+</sup> cells after 20 weeks and calculated as 1 per 12 (95% confidence interval 1 in 6 to 1 in 23, Figure 4B). This multilineage engraftment frequency is significantly higher than that of endosteal LSK transplanted in a limiting dilution transplantation assay without prior functional enrichment (frequency 1:259, 95% confidence interval 1 in 175 to 1 in 381,  $n = 4$ ). Our data demonstrate, for the first time, that LT-HSCs preferentially migrate to the endosteum within 5 hours after transplantation, and this provides a valuable tool for their selection.

### Blocking CD48 significantly reduces LSK homing efficiency

As described in "CD150<sup>+</sup>CD48<sup>-</sup> LSK harvested from endosteal BM have the highest homing efficiency," LSK that are not

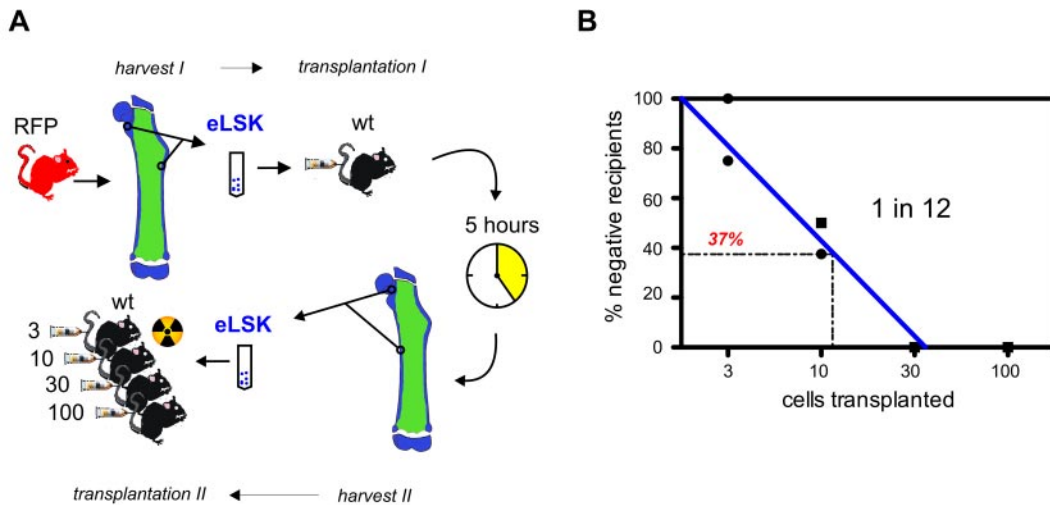


**Figure 4. Functional selection of HSCs.** (A) RFP<sup>+</sup> endosteal LSK were transplanted into 1 nonablated recipient. After 5 hours, LSK homed to endosteal BM were reisolated and transplanted into ablated secondary recipients in a limiting dilution assay. (B) Limiting dilution analysis of 2 experiments. Each symbol represents a group of mice transplanted with 3, 10, 30, or 100 cells.

CD150<sup>+</sup>CD48<sup>-</sup> (Figure 3A blue sort region) have significantly reduced homing efficiency compared with total LSK (Figure 3B). To understand this unexpected paradox, we analyzed the role of CD41 and CD48 in homing. Flow cytometric analysis of the expression of CD41 and CD48 on endosteal and central LSK demonstrated that the majority of cells expressed CD48 (~86%), few express CD41 (~7%), and more than 90% of CD41<sup>+</sup> cells also expressed CD48 (Figure 5A). There were no differences in the expression levels of the 2 surface proteins on endosteal or central LSK (data not shown).

Analysis of the homing efficiency of LSK labeled with antibodies to, but not sorted on, the basis of CD48 or CD41 was performed by cotransplanting endosteal and central populations. As seen in Figure 5B, no change in homing in the presence of CD41 antibody was detected. However, cells labeled with anti-CD48 (HM48.1 clone, widely used in studies describing CD48<sup>+</sup> cells) had a significant decrease in homing efficiency compared with unstained LSK (8% ± 3% and 21% ± 2%,  $P < .005$ ; and 8% ± 4% and 17% ± 1%,  $P < .05$  for endosteal and central LSK, respectively). In contrast, the use of an alternate CD48 antibody (OX-78 clone) demonstrated no significant change in the homing ability of transplanted CD48 labeled cells compared with unlabeled LSK regardless of the BM region from which they were isolated ( $P > .05$ ). These data suggest that CD48 is important in LSK homing after transplantation and that antibodies used for positive selection influence their functional properties.

Importantly, even when the OX-78 CD48 antibody clone was used, endCD150<sup>+</sup>CD48<sup>-</sup> LSK exhibited the highest homing efficiency of all LSK subpopulations (data not shown). In contrast, centCD150<sup>+</sup>CD48<sup>-</sup> LSK had no homing advantage, compared with total central LSK (Figure 3B).

As long-term engraftment studies involve transplantations into ablated recipients, the homing efficiency of LSK with and without prior staining with CD48 (HM48.1 clone) was also compared 15 hours after transplantation into irradiated recipients. Similarly to transplantations into nonablated recipients, significantly less LSK homed to BM after labeling with CD48 (HM48.1) compared with unstained LSK (6% ± 2% and 16% ± 2% and 7% ± 2% and 16% ± 1% for endosteal and central LSK, respectively;  $P < .005$ ; Figure 5C). This strongly suggests that a specific interaction

between CD48 and endothelial cells is still required for homing after ablation.

As blocking CD48 significantly reduced homing efficiency, we analyzed whether blocking CD48 also altered trans-marrow migration and lodgment. CD48-labeled and unlabeled LSK were transplanted into ablated and nonablated recipients and their spatial distribution in BM analyzed 15 hours after transplantation. After a transplantation of endosteal and central LSK into nonablated recipients, 65% ± 2% and 51% ± 12%, respectively, were located in endosteal BM (Figure 5D), previously defined as 12 cell diameters from the bone/BM interface.<sup>27</sup> Pretransplantation irradiation of recipients resulted in a significant increase in the percentage of endosteal and central LSK (84% ± 5% and 88% ± 7%, respectively) lodging within endosteal BM (Figure 5E,  $P < .05$ ). No significant differences ( $P > .05$ ) in spatial distribution were detected when CD48-labeled LSK were transplanted into nonablated or ablated recipients (Figure 5D and Figure 5E, respectively). This suggests that, although CD48 may be important for cells homing to BM, it is not critical for trans-marrow migration and lodgment.

Based on our observation that CD48 is involved in HSPC homing, we conducted a series of in vivo experiments to further characterize the hemopoietic potential of CD48<sup>+/-</sup> HSPCs.

#### Endosteal and central CD150<sup>+</sup>CD48<sup>+</sup> LSK have lower engraftment potential than CD150<sup>+</sup>CD48<sup>-</sup> LSK

The in vivo hemopoietic potential of CD150<sup>+</sup>CD48<sup>+</sup> LSK and CD150<sup>+</sup>CD48<sup>-</sup> LSK was compared using competitive transplantations of endosteal and central BM. Previous reports suggest that CD48<sup>+</sup> BM is devoid of multilineage engraftment potential.<sup>6,28</sup> However, these studies used function blocking CD48 antibody, which decreases homing efficiency 3-fold (Figures 3B, 5B). As a consequence, we hypothesize that the frequency of repopulating cells within CD48<sup>+</sup> LSK homing to BM when selected using this antibody would be too low for detection. Using nonblocking CD48 antibody (OX-78 clone), 200 or 150 RFP CD150<sup>+</sup>CD48<sup>-</sup> LSK were competed with 500, 200, 100, or 20 PTPRCA CD150<sup>+</sup>CD48<sup>+</sup> LSK, with both phenotypes isolated from either endosteal or central BM (Figure 6A). Overall survival was more than 85% for all recipients (Figure 6B). Analysis of recipient PB nucleated cells (PBNCs) after 5 weeks revealed more than 40%

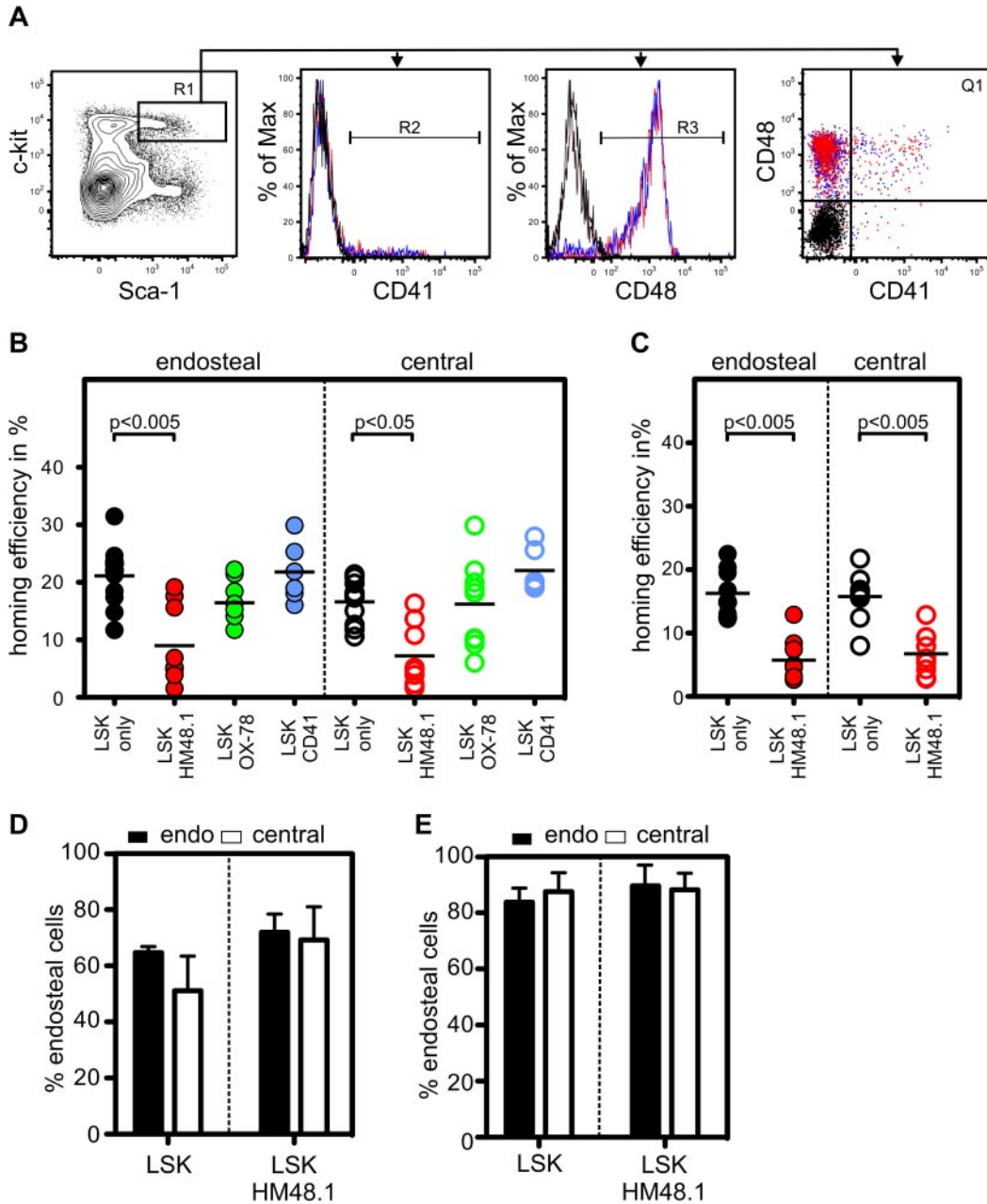


**Figure 5. Role of CD48 in HSPC homing.** (A) Representative analysis of CD41 (R2) and CD48 (R3) expression on endosteal and central LSK. Black represents isotype control; red, endosteal LSK; and blue, central LSK. (B) Unsorted endosteal and central LSK were cotransplanted with endosteal and central LSK, labeled with CD48 (HM48.1 clone), CD48 (OX-78 clone), or CD41 antibody but not sorted on the basis of their expression, and the homing efficiency analyzed 15 hours after transplantation into nonablated and (C) ablated recipients. (D) Spatial distribution of LSK or LSK stained with CD48 (HM48.1) 15 hours after transplantation into nonablated and ablated (E) recipients. (B-C) Dot graphs: Each dot represents an individual recipient; line represents the mean. (D-E) Bar graphs: At least 50 cells from 6 sections from 3 individual recipients were analyzed. Data are mean  $\pm$  SEM.

donor contribution from either end or centCD150<sup>+</sup>CD48<sup>-</sup>LSK. After 20 weeks, the proportion of donor PBNCs from CD150<sup>+</sup>CD48<sup>-</sup>LSK increased to 87% (range, 78%-96% and 67%-94% from endosteal and central BM, respectively; Figure 6C-D). In contrast, the contribution of either end or centCD150<sup>+</sup>CD48<sup>+</sup>LSK progeny was very low, with an average of 3% donor PBNCs detected 5 weeks after a cotransplantation of 500 CD150<sup>+</sup>CD48<sup>+</sup>LSK with 200 CD150<sup>+</sup>CD48<sup>-</sup>LSK, and this decreased after 20 weeks (Figure 6C-D).

Analysis of the proportion of donor myeloid and lymphoid cells (Figure 6E-F) demonstrated that 5 weeks after transplanting CD150<sup>+</sup>CD48<sup>-</sup>LSK, the majority of donor PBNCs were Gr-1/Mac-1<sup>+</sup>

(range, 20%-89% and 37%-94% for endosteal and central BM, respectively). This contribution decreased to 6% to 38% and 3% to 22% 20 weeks after transplantation. The percentage of B220<sup>+</sup> PB cells increased over time from 27% and 23% (range, 3%-71% and 2%-52%) after 5 weeks to 57% and 53% (range, 35%-66% and 25%-76%) after 20 weeks for endosteal and central donor cells, respectively. The same trend was evident for CD3<sup>+</sup> cells.

In contrast, the progeny of CD150<sup>+</sup>CD48<sup>+</sup>LSK had a different and highly variable lineage distribution compared with the progeny of CD150<sup>+</sup>CD48<sup>-</sup>LSK (Figure 6G-H). Five weeks after a transplantation of 500 CD150<sup>+</sup>CD48<sup>+</sup>LSK, 51% and 43% (range, 10%-80% and 27%-92% for endosteal and central origin, respectively) were

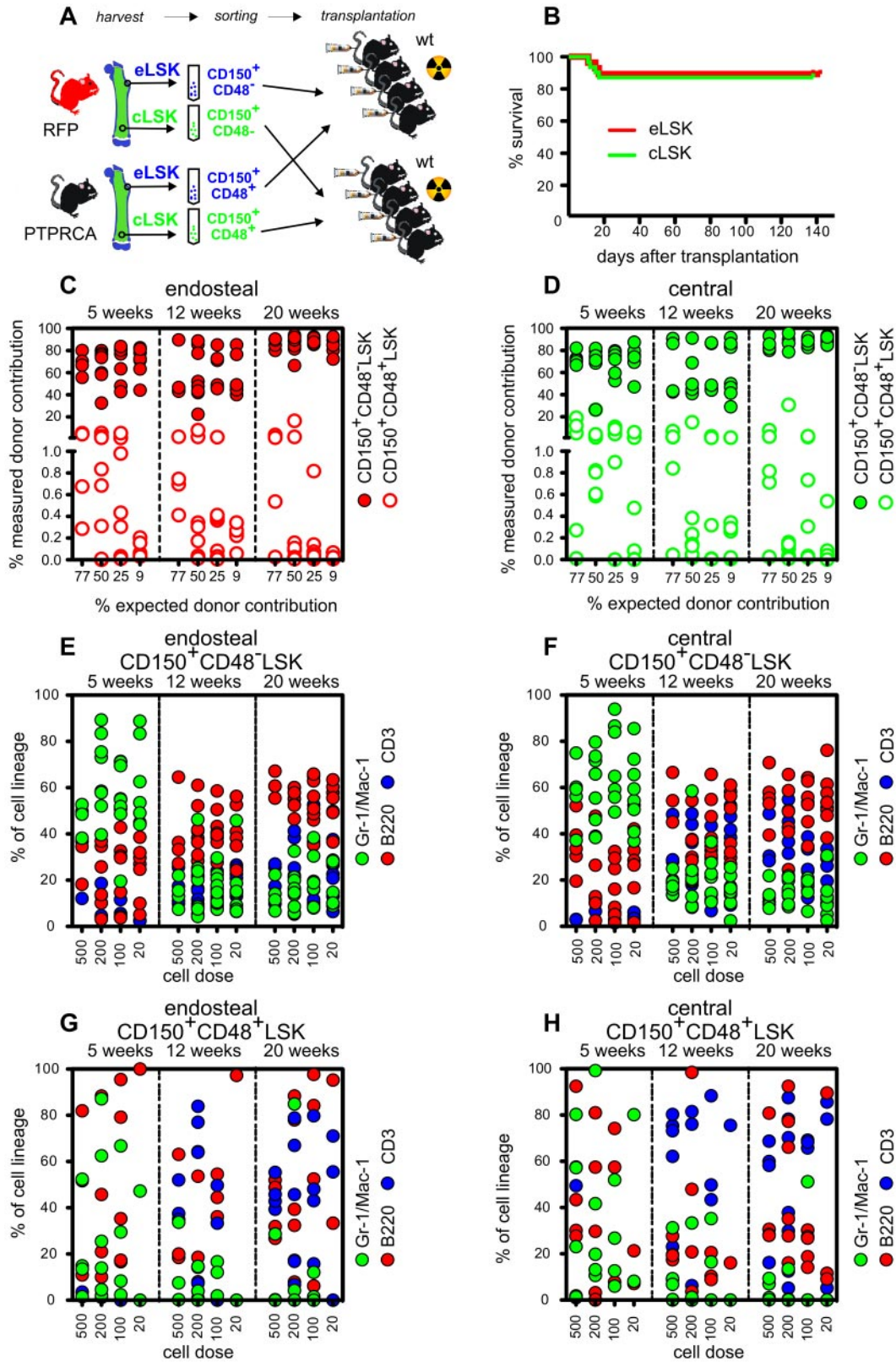


**Figure 6. Endosteal and central CD150<sup>+</sup>CD48<sup>-</sup>LSK reconstitute and out-compete CD150<sup>+</sup>CD48<sup>+</sup>LSK.** (A) Endosteal and central CD150<sup>+</sup>CD48<sup>-</sup>LSK were transplanted in a competitive limiting dilution assay with CD150<sup>+</sup>CD48<sup>+</sup>LSK from the same BM region. (B) Survival of lethally irradiated recipients. (C) Graph shows percentage of BM reconstitution from CD150<sup>+</sup>CD48<sup>-</sup>LSK from endosteal and (D) central BM. (E) Plot shows lymphoid and myeloid progeny of endosteal and (F) central CD150<sup>+</sup>CD48<sup>-</sup>LSK. Both transplanted cell populations show physiologic multilineage reconstitution after 20 weeks. (G) Plot shows lymphoid and myeloid progeny of endosteal and (H) central CD150<sup>+</sup>CD48<sup>+</sup>LSK. Each dot represents individual recipients from 2 independent transplantations.

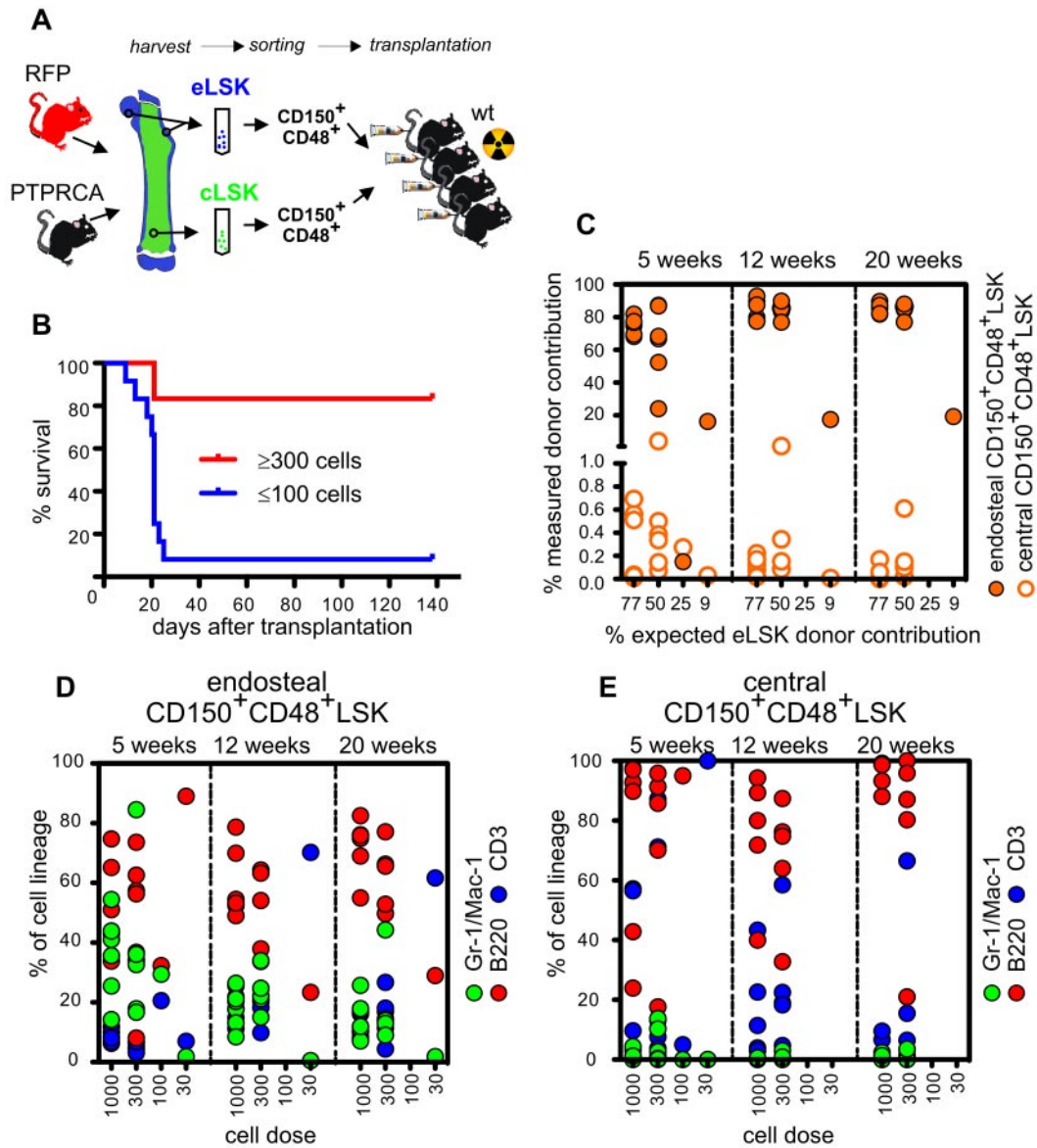


**Figure 7. Endosteal, but not central,  $CD150^{+}CD48^{+}LSK$  have multilineage engraftment potential.** (A) Endosteal and central  $CD150^{+}CD48^{+}LSK$  were transplanted in a competitive limiting dilution assay. (B) Survival of lethally irradiated recipients. (C) Graph shows percentage of progeny of endosteal (●) and central (○)  $CD150^{+}CD48^{+}LSK$ . (D) Graph shows lymphoid and myeloid progeny of endosteal  $CD150^{+}CD48^{+}LSK$ :  $> 1:300$  endosteal  $CD150^{+}CD48^{+}LSK$  show physiologic multilineage reconstitution. (E) Graph shows lymphoid (red and purple circles) and myeloid (green circles) progeny of central  $CD150^{+}CD48^{+}LSK$ : Central  $CD150^{+}CD48^{+}LSK$  exhibit low levels of lymphoid but are devoid of myeloid progeny. Each dot represents individual recipients.

$B220^{+}$  (Figure 6E-F). The numbers of  $Gr-1/Mac-1^{+}$  cells were also lower (average of 14% and 23%; range, 2%-52% and 1%-80% for endosteal and central donor BM, respectively). After 20 weeks, the number of  $Gr-1/Mac-1^{+}$  cells further decreased ( $< 5\%$ ), and nearly all progeny of transplanted  $CD150^{+}CD48^{+}LSK$  in the PB were lymphoid.

#### A subset of endosteal $CD150^{+}CD48^{+}LSK$ have multilineage reconstitution potential

The low levels of engraftment observed with  $CD150^{+}CD48^{+}LSK$  after competitive transplantations with  $CD150^{+}CD48^{+}LSK$  could either be the result of this phenotype lacking multilineage reconstitution potential or the cells being out-competed. Therefore, we performed limiting dilution transplantations competing 1000, 300, 100, or 30 endosteal  $CD150^{+}CD48^{+}LSK$  with 300 central  $CD150^{+}CD48^{+}LSK$  (Figure 7A). A total of 80% of

transplantation recipients receiving more than or equal to 300 endosteal cells survived 20 weeks after transplantation (Figure 7B). After 5 weeks, PB analysis demonstrated that 76% and 68% (range, 68%-82% and 24%-87%) PBNCs were the progeny of 1000 and 300 transplanted endosteal  $CD150^{+}CD48^{+}LSK$ , respectively, increasing to 86% and 85% (range, 82%-90% and 77%-88%) after 20 weeks (Figure 7C). The contribution of 300 central  $CD150^{+}CD48^{+}LSK$  was always less than 2%, suggesting that these cells, phenotypically identical for  $CD150^{+}CD48^{+}LSK$ , have significantly reduced reconstitution potential compared with their endosteal counterparts.

Analysis of the progeny of 1000 and 300 transplanted endosteal  $CD150^{+}CD48^{+}LSK$  showed that 38% and 33% (range, 14%-54% and 16%-85%) were myeloid ( $Gr-1/Mac-1^{+}$ ) and 48% and 57% (range, 34%-75% and 8%-74%) were lymphoid ( $B220^{+}$ ), respectively, after 5 weeks (Figure 7D), suggesting a higher

percentage of short-term lymphoid engrafting cells compared with CD150<sup>+</sup>CD48<sup>-</sup>LSK (Figure 6E).

However, mice transplanted with endCD150<sup>+</sup>CD48<sup>+</sup>LSK showed a similar proportion of both myeloid and lymphoid cells in the PB to those transplanted with endCD150<sup>+</sup>CD48<sup>-</sup>LSK after 20 weeks (Figures 6E, 7D). The calculation of long-term multilineage reconstituting cells within the CD150<sup>+</sup>CD48<sup>+</sup>LSK fraction was based on the Poisson distribution using the program L-Calc and was 1 in 289. This frequency, however, is significantly lower than for CD150<sup>+</sup>CD48<sup>-</sup>LSK cells.<sup>6</sup>

In contrast, after 20 weeks, centCD150<sup>+</sup>CD48<sup>+</sup>LSK contribution was less than 1% (Figure 7C), and more than 70% of these cells were lymphoid (Figure 7E). Together with *in vitro* proliferation data (Figure 2B), this suggests that centCD150<sup>+</sup>CD48<sup>+</sup>LSK contain cells capable of lymphoid, but not myeloid, reconstitution potential.

Collectively, the data demonstrate that HSPC location correlates with and potentially predicts functional properties, suggesting that extrinsic regulatory processes within endosteal BM determines hemopoietic potential.

## Discussion

The existence of a HSC niche was proposed 30 years ago,<sup>29</sup> but only recent advances in phenotypic HSC purification and improved visualization techniques have enabled thorough assessment of the localization of HSCs within BM. To date, few data describe differences in function of HSPCs isolated from different hemopoietic microenvironments. Recently, however, we provided evidence that endosteal HSPCs have increased *in vivo* hemopoietic reconstitution potential compared with central HSPCs.<sup>22</sup> In this study, we extend these findings, demonstrating that HSCs, CD150<sup>+</sup>CD48<sup>-</sup>LSK, have considerably different biologic properties depending on their BM region of origin.

Hemopoietic reconstitution occurs when infused HSCs home and engraft within BM, a process involving 4 steps: adhesion to vascular endothelium, trans-endothelial migration, trans-marrow migration, and lodgment in the HSC niche. HSCs express many cell adhesion molecules (CAMs) and chemokine receptors, enabling them to specifically home to their niche during engraftment.<sup>30</sup> Although the analysis of reconstitution potential of defined HSC subpopulations is the gold standard for assessing hemopoietic potential, careful analysis of the components of engraftment and specifically the efficiency of homing is often overlooked. Our studies and those of others demonstrate that altered CAM expression or function influences homing efficiency. For example, blocking or up-regulating  $\alpha_4\beta_1$  integrin on HSCs significantly reduces or increases homing efficiency, respectively.<sup>31,32</sup> Most importantly, changes in homing affect the observed frequency of engrafting cells (multilineage LT-HSCs) in limiting dilution transplantations. This suggests that endosteal HSCs have as yet undetermined differences in CAM expression and or function to their central counterparts, enabling them to home more efficiently.

Our study highlights the novel role of CD48 in HSPC homing. CD48 is a GPI-linked cell surface molecule expressed by leukocytes and known to be involved in T-cell proliferation and activation.<sup>33</sup> CD48 binds homophilically and to other members of its receptor family, including CD2, CD244, and CD58. Spatial distribution analysis of CD48<sup>+</sup>LSK after transplantation did not show cells actively trans-endothelially migrating, suggesting reduced adhesion to the endothelial wall. Although we cannot

exclude complement activation and lysis of HM48.1-labeled LSK, there is no evidence in the literature suggesting this as a mechanism. In addition, previous studies demonstrate that blocking CD244 binding to CD48 with HM48.1 antibody interrupts T and NK cell interactions,<sup>34</sup> further demonstrating this antibody as function blocking.

The significance of CD48 on HSPCs was described by Kiel et al<sup>6</sup> and Kim et al<sup>28</sup> who showed that transplanting CD48<sup>+</sup> whole bone marrow (WBM) results in only lymphoid progenitor engraftment. In addition, CD48<sup>+</sup> and CD48<sup>+</sup>CD135<sup>-</sup>LSK transplantations showed no detectable multilineage engraftment. CD48 expression was suggested to be exclusive to colony-forming progenitors, not HSC or multipotent progenitors. These studies were conducted using BM isolated by traditional flushing techniques and are in accord with our results using centCD150<sup>+</sup>CD48<sup>+</sup>LSK. However, as endCD150<sup>+</sup>CD48<sup>+</sup>LSK would not have been assessed, the long-term multilineage reconstituting cells we have now identified within this region with this phenotype would not have previously been detected.

In addition, the studies described herein used the HM48.1 antibody clone to isolate CD48<sup>+</sup> HSPCs and conclude that these cells are not capable of long-term multilineage engraftment. Critically, our data demonstrate that less than 10% of endosteal or centCD150<sup>+</sup>CD48<sup>+</sup>LSK home to BM when selected using this clone. This is in distinct contrast to using the OX-78 CD48 antibody clone, which has no impact on cell homing. These data highlight the importance of assessing homing efficiency as part of reconstitution potential analysis. In this case, failure to recognize that selecting CD48<sup>+</sup> HSPCs using the HM48.1 antibody clone would have resulted in less than 50% and less than 30% of the normal level of homing for this phenotype isolated from central and endosteal BM, respectively. Consequently, the reconstitution potential of these cells would have been vastly underestimated or not detected.

Only 1 previous study used the OX78 CD48 clone for isolating CD48<sup>+</sup> BM and assessing their reconstitution ability after transplantation.<sup>35</sup> However, the BM isolation method was not described and did not separately assess endosteal and central BM. In addition, HSPCs were phenotypically defined as Lin<sup>-</sup>CD150<sup>+</sup>CD48<sup>+</sup> without including Sca and c-Kit, representing a very heterogeneous population, of which only a minority of cells would be CD150<sup>+</sup>CD48<sup>+</sup>LSK. As a consequence, it is unlikely that the endCD150<sup>+</sup>CD48<sup>+</sup>LSK with long-term multilineage reconstitution potential described in our study would be evident in their readout. Our study did not detect multilineage reconstitution from transplanted centCD150<sup>+</sup>CD48<sup>+</sup>LSK but did demonstrate lymphoid potential.

The *in vivo* lymphoid commitment of centCD150<sup>+</sup>CD48<sup>+</sup>LSK was mirrored in our *in vitro* experiments. After stimulation with a combination of early acting cytokines,<sup>36</sup> a significantly lower proliferative response was evident in centCD150<sup>+</sup>CD48<sup>-</sup>LSK, and most nascent Sca<sup>+</sup>c-Kit<sup>+</sup> cells were generated from endCD150<sup>+</sup>CD48<sup>-</sup>LSK. This suggests that CD150<sup>+</sup>CD48<sup>-</sup>LSK in close proximity to bone are more sensitive to early acting cytokines or are intrinsically different from central CD150<sup>+</sup>CD48<sup>-</sup>LSK. In addition, CD150<sup>+</sup>CD48<sup>+</sup>LSK generated significantly more B220<sup>+</sup> progeny, an outcome to be expected for a cell subpopulation enriched for lymphoid committed progenitors.

Studies with common lymphoid and myeloid progenitors defined as Lin<sup>-</sup>Sca-1<sup>lo</sup>c-kit<sup>lo</sup>IL-7R $\alpha$ <sup>+</sup> and Lin<sup>-</sup>Sca<sup>-</sup>c-kit<sup>-</sup>IL-7R $\alpha$ <sup>-</sup> confirm IL-7R $\alpha$  expression as a marker for B-cell development.<sup>26</sup> In this study, we demonstrate (Figure 2D) that IL-7R $\alpha$  is not

expressed on CD150<sup>+</sup>CD48<sup>-</sup>LSK, whereas a subset of CD150<sup>+</sup>CD48<sup>+</sup>LSK express IL7R $\alpha$  and cells of this phenotype isolated from central BM express twice as much IL-7R $\alpha$  than their endosteal counterparts. This suggests that a subset of CD150<sup>+</sup>CD48<sup>+</sup>LSK is primed for lymphoid differentiation even while expressing high levels of c-kit. The stimulation of IL-7R $\alpha$ <sup>+</sup>CD150<sup>+</sup>CD48<sup>+</sup>LSK with IL-11, FL, and SCF in culture is in accord with previously described effects of these cytokines on B-cell development.<sup>37</sup>

Furthermore, we show that approximately 25% of total CD150<sup>+</sup>CD48<sup>-</sup>LSK are located in endosteal BM and can be isolated using a previously published method involving grinding and digestion of flushed bones.<sup>22</sup> This HSC isolation method is critical, as traditional BM collection methods of flushing alone result in endosteal HSCs being discarded. Moreover, endosteal HSCs have significantly higher hemopoietic potential compared with their central counterparts.

In conclusion, we show that endCD150<sup>+</sup>CD48<sup>-</sup>LSK exhibit considerably different biologic properties to their phenotypically identical central BM counterparts, suggesting that they are only truly phenotypically identical in relation to their expression of CD150CD48LSK. EndCD150<sup>+</sup>CD48<sup>-</sup>LSK show higher proliferative potential in vitro and an increased homing efficiency in vivo. In addition, we demonstrate that a subset of endCD150<sup>+</sup>CD48<sup>+</sup>LSK have a previously unrecognized long-term multilineage reconstitution potential, provided a nonfunction blocking antibody is used for their isolation. Overall, our data suggest a hierarchical relationship of HSPC subsets with identical CD150CD48LSK phenotypic characteristics isolated from different BM regions. These biologic differences could be attributed to combinations of intrinsic differ-

ences as well as unique extrinsic cues conferred by their microenvironment of origin. Transcriptional and proteomic profiling studies of these 2 functionally distinct populations are currently being performed within our laboratory to identify and characterize these differences.

## Acknowledgments

The authors thank Daniela Cardozo and Kate Rutherford for help with animal work and Andrew Fryga, Darren Ellemor, Kathryn Flanagan, and Karen Yuen for flow cytometric support.

This work was supported by the German Cancer Aid (Deutsche Krebshilfe; J.G.) and the Australian Stem Cell Centre (S.K.N., D.N.H.).

## Authorship

Contribution: J.G. and S.K.N. designed and performed experiments, analyzed data, and wrote the manuscript; D.N.H. designed experiments, analyzed data, and wrote the manuscript; and B.W. and G.H.O. performed experiments.

Conflict-of-interest disclosure: The authors declare no competing financial interests.

Correspondence: Susan K. Nilsson, Commonwealth Scientific and Industrial Research Organisation, c/o Australian Stem Cell Centre, 3rd Fl, Bldg 75 (STRIP), Monash University, Wellington Rd, Clayton, Victoria, 3800, Australia; e-mail: susie.nilsson@csiro.au.

## References

- Yin T, Li L. The stem cell niches in bone. *J Clin Invest*. 2006;116(5):1195-1201.
- Kondo M, Wagers AJ, Manz MG, et al. Biology of hematopoietic stem cells and progenitors: implications for clinical application. *Annu Rev Immunol*. 2003;21:759-806.
- Spangrude GJ, Aihara Y, Weissman IL, Klein J. The stem cell antigens SCA-1 and SCA-2 subdivide thymic and peripheral T lymphocytes into unique subsets. *J Immunol*. 1988;141(11):3697-3707.
- Osawa M, Hanada K, Hamada H, Nakauchi H. Long-term lymphohematopoietic reconstitution by a single CD34-low/negative hematopoietic stem cell. *Science*. 1996;273(5272):242-245.
- Christensen JL, Weissman IL. Flk-2 is a marker in hematopoietic stem cell differentiation: a simple method to isolate long-term stem cells. *Proc Natl Acad Sci U S A*. 2001;98(25):14541-14546.
- Kiel MJ, Yilmaz OH, Iwashita T, Terhorst C, Morrison SJ. SLAM family receptors distinguish hematopoietic stem and progenitor cells and reveal endothelial niches for stem cells. *Cell*. 2005;121(7):1109-1121.
- Diessen RL, Johnston HM, Nilsson SK. Membrane-bound stem cell factor is a key regulator in the initial lodgment of stem cells within the endosteal marrow region. *Exp Hematol*. 2003;31(12):1284-1291.
- Nilsson SK, Haylock DN, Johnston HM, Oochiodoro T, Brown TJ, Simmons PJ. Hyaluronan is synthesized by primitive hemopoietic cells, participates in their lodgment at the endosteum following transplantation, and is involved in the regulation of their proliferation and differentiation in vitro. *Blood*. 2003;101(3):856-862.
- Calvi LM, Adams GB, Weibrecht KW, et al. Osteoblastic cells regulate the haematopoietic stem cell niche. *Nature*. 2003;425(6960):841-846.
- Zhang J, Niu C, Ye L, et al. Identification of the haematopoietic stem cell niche and control of the niche size. *Nature*. 2003;425(6960):836-841.
- Arai F, Hiraio A, Ohmura M, et al. Tie2/angiopoietin-1 signaling regulates hematopoietic stem cell quiescence in the bone marrow niche. *Cell*. 2004;118(2):149-161.
- Jung Y, Wang J, Havens A, Sun Y, Jin T, Taichman RS. Cell-to-cell contact is critical for the survival of hematopoietic progenitor cells on osteoblasts. *Cytokine*. 2005;32(3):155-162.
- Nilsson SK, Johnston HM, Whitty GA, et al. Osteopontin, a key component of the hematopoietic stem cell niche and regulator of primitive hematopoietic progenitor cells. *Blood*. 2005;106(4):1232-1239.
- Adams GB, Chabner KT, Alley IR, et al. Stem cell engraftment at the endosteal niche is specified by the calcium-sensing receptor. *Nature*. 2006;439(7076):599-603.
- Parmar K, Mauch P, Vergilio JA, Sackstein R, Down JD. Distribution of hematopoietic stem cells in the bone marrow according to regional hypoxia. *Proc Natl Acad Sci U S A*. 2007;104(13):5431-5436.
- Levesque JP, Winkler IG, Hendy J, et al. Hematopoietic progenitor cell mobilization results in hypoxia with increased hypoxia-inducible transcription factor-1 alpha and vascular endothelial growth factor A in bone marrow. *Stem Cells*. 2007;25(8):1954-1965.
- Nie Y, Han YC, Zou YR. CXCR4 is required for the quiescence of primitive hematopoietic cells. *J Exp Med*. 2008;205(4):777-783.
- Grassinger J, Haylock DN, Storan MJ, et al. Thrombin-cleaved osteopontin regulates hemopoietic stem and progenitor cell functions through interactions with alpha9beta1 and alpha4beta1 integrins. *Blood*. 2009;114(1):49-59.
- Chan CK, Chen CC, Luppen CA, et al. Endochondral ossification is required for haematopoietic stem-cell niche formation. *Nature*. 2009;457(7228):490-494.
- Lo Celso C, Fleming HE, Wu JW, et al. Live-animal tracking of individual haematopoietic stem/progenitor cells in their niche. *Nature*. 2009;457(7225):92-96.
- Xie Y, Yin T, Wiegand W, et al. Detection of functional haematopoietic stem cell niche using real-time imaging. *Nature*. 2009;457(7225):97-101.
- Haylock DN, Williams B, Johnston HM, et al. Hemopoietic stem cells with higher hemopoietic potential reside at the bone marrow endosteum. *Stem Cells*. 2007;25(4):1062-1069.
- Grassinger J, Nilsson SK. Methods to analyze the homing efficiency and spatial distribution of hematopoietic stem and progenitor cells and their relationship to the bone marrow endosteum and vascular endothelium. In: *Methods in Molecular Biology*. Clifton, NJ: ;2010.
- Nilsson SK, Johnston HM, Coverdale JA. Spatial localization of transplanted hemopoietic stem cells: inferences for the localization of stem cell niches. *Blood*. 2001;97(8):2293-2299.
- Bradford GB, Williams B, Rossi R, Bertonecchio I. Quiescence, cycling, and turnover in the primitive hematopoietic stem cell compartment. *Exp Hematol*. 1997;25:445-453.
- Kondo M, Weissman IL, Akashi K. Identification of clonogenic common lymphoid progenitors in mouse bone marrow. *Cell*. 1997;91(5):661-672.
- Nilsson SK, Dooner MS, Tiarks CY, Weier H-U, Quesenberry PJ. Potential and distribution of transplanted hematopoietic stem cells in a nonablated mouse model. *Blood*. 1997;89(11):4013-4020.

28. Kim I, He S, Yilmaz OH, Kiel MJ, Morrison SJ. Enhanced purification of fetal liver hematopoietic stem cells using SLAM family receptors. *Blood*. 2006;108(2):737-744.
29. Schofield R. The relationship between the spleen colony-forming cell and the haemopoietic stem cell. *Blood Cells*. 1978;4(1):7-25.
30. Nilsson SK, Simmons PJ. Transplantable stem cells: home to specific niches. *Curr Opin Hematol*. 2004;11(2):102-106.
31. Papayannopoulou T, Craddock C, Nakamoto B, Priestley GV, Wolf NS. The VLA4/VCAM-1 adhesion pathway defines contrasting mechanisms of lodgement of transplanted murine hemopoietic progenitors between bone marrow and spleen. *Proc Natl Acad Sci U S A*. 1995;92(21):9647-9651.
32. Wagers AJ, Allsopp RC, Weissman IL. Changes in integrin expression are associated with altered homing properties of Lin(-)Thy1.1(lo)Sca-1(+)c-kit(+) hematopoietic stem cells following mobilization by cyclophosphamide/granulocyte colony-stimulating factor. *Exp Hematol*. 2002;30(2):176-185.
33. Yokoyama S, Staunton D, Fisher R, Amiot M, Fortin JJ, Thorley-Lawson DA. Expression of the Blast-1 activation/adhesion molecule and its identification as CD48. *J Immunol*. 1991;146(7):2192-2200.
34. McNerney ME, Lee KM, Kumar V. 2B4 (CD244) is a non-MHC binding receptor with multiple functions on natural killer cells and CD8+ T cells. *Mol Immunol*. 2005;42(4):489-494.
35. McKinney-Freeman SL, Naveiras O, Yates F, et al. Surface antigen phenotypes of hematopoietic stem cells from embryos and murine embryonic stem cells. *Blood*. 2009;114(2):268-278.
36. Nakauchi H, Sudo K, Ema H. Quantitative assessment of the stem cell self-renewal capacity. *Ann N Y Acad Sci*. 2001;938:18-24, discussion 24-25.
37. Lemieux ME, Chappel SM, Miller CL, Eaves CJ. Differential ability of flt3-ligand, interleukin-11, and Steel factor to support the generation of B cell progenitors and myeloid cells from primitive murine fetal liver cells. *Exp Hematol*. 1997;25(9):951-957.